

## A Novel Large Conductance, Nonselective Cation Channel in Pheochromocytoma (PC12) Cells

A.M. Dopico, S.N. Treistman

Department of Pharmacology and Molecular Toxicology, and Program in Neuroscience, University of Massachusetts Medical School, 55 Lake Avenue North, Worcester, MA 01655, USA

Received: 14 February 1997/Revised: 28 July 1997

**Abstract.** A new type of nonselective cation channel was identified and characterized in pheochromocytoma (PC12) cells using inside-out and cell-attached patch-clamp recordings. The channel shows a large unitary conductance (274 pS in symmetric 145 mM  $K^+$ ) and selectivity for  $Na^+ \approx K^+ > Li^+$ , and is practically impermeable to  $Cl^-$ . The channel activity-voltage relationship is bell-shaped, showing maximal activation at  $\approx -10$  mV. The overall activity of this channel is unmodified by  $[Na^+]_{ic}$ , or  $[Ca^{++}]_{ic}$ . However, increases in  $[Ca^{++}]_{ic}$  lead to a decrease in the unitary current amplitude. In addition, overall activity is mildly increased when suction is applied to the back of the patch pipette. Together, these characteristics distinguish the present channel from all other large conductance nonselective cation channels reported so far in a variety of preparations. The frequency of appearance of this channel type is similar in undifferentiated and NGF-treated PC12 cells ( $\approx 8$ –27% of patches). The combination of large conductance, permeability to  $Na^+$ , and existence of conducting states at negative potentials, may provide a significant pathway for inward current and depolarization in PC12 cells.

**Key words:** Patch clamp — Nonselective cation channel — PC12 cells — NGF — Stretch-activation — Cytosolic  $Ca^{++}$

### Introduction

PC12 cells constitute a neurosecretory cell line derived from a pheochromocytoma of the rat adrenal medulla

(Greene & Tischler, 1976). Using whole-cell and/or single channel current recordings, a wide variety of ion channel populations have been identified in this clonal cell line, including L- and N-type voltage-gated  $Ca^{++}$  channels, several classes of both purely voltage-gated  $K^+$  channels and  $Ca^{++}$ -dependent  $K^+$  channels, both tetrodotoxin-sensitive and insensitive  $Na^+$  channels (for a review, *see* Shafer & Atchison, 1991) and, more recently, nicotinic acetylcholine receptor channels (Sands & Barish, 1992), and ATP-gated (P2x purinoreceptors) cation channels (Evans et al., 1995).

Nerve growth factor (NGF) induces differentiation of PC12 cells from chromaffin-like cells to sympathetic neuron-like cells. This process is evident after several days of exposure to NGF, which results in neurite outgrowth (Greene & Tischler, 1976). NGF-induced differentiation of PC12 cells is accompanied by up- or down-regulation of ion channels populations, such as  $Na^+$  channels (Pollock, Krempin, & Rudy, 1990; Fanger et al., 1995),  $Ca^{++}$  channels (Streit & Lux, 1987; Garber, Hoshi, & Aldrich, 1989; Lewis, De Aizpurua & Rausch, 1993; Tewari et al., 1995), nicotinic acetylcholine receptor channels (Fanger et al., 1995) and, possibly, small conductance,  $Ca^{++}$ -activated  $K^+$  channels (Schmid-Antomarchi, Hugues, & Lazdunski, 1986). The study of both the changes in channel expression after NGF-induced differentiation, and the action of physiological modulators or pharmacological agents on these conductances (Mullikin-Kilpatrick & Treistman, 1995), as well as the characterization of the ion channel populations themselves, have made of PC12 cells a model system widely used in neurobiology.

The degree of ion selectivity of ion channel populations is an important criterion for their classification. Nonselective cation channels are a largely heterogenous group (for a review, *see* Siemen, 1993). In a broad

sense, we may include the nicotinic acetylcholine receptor, glutamate-receptor channels, cyclic nucleotide-gated-channels, ATP-activated cationic channels, bacterial porins, arginine-dependent channels, channels involved in taste perception, the voltage-dependent anion channel (VDAC) and related channels, such as major intrinsic protein (MIP) channels, under particular ionic conditions, and the subgroup of  $\text{Ca}^{++}$ -dependent nonselective cation channels,  $\text{Na}^+$ -activated cationic channels, and mechano-gated cationic channels. Whereas in a few cases both detailed electrophysiological properties and kinetic schemes, as well as the molecular biology (even topology) of the channel are known, as in the case of the nicotinic acetylcholine receptor of the neuromuscular plate, in others, such as with most mechanosensitive cation channels, such knowledge is not available.

In the present communication, we report the existence of a new type of nonselective cation channel, found in both undifferentiated and NGF-treated PC12 cells. This channel is equally permeable to  $\text{Na}^+$  and  $\text{K}^+$ , and has a large unitary conductance ( $\approx 274$  pS in 145 mM  $\text{K}^+$ ), which is decreased as  $[\text{Ca}^{++}]_{ic}$  is increased. Its activity is modified by transmembrane voltage, resulting in a bell-shaped relationship, and also mildly increased when negative pressure is applied to the back of the patch pipette. On the other hand, overall activity is not affected by changes in either  $[\text{Ca}^{++}]_{ic}$  or  $[\text{Na}^+]_{ic}$ . Although the physiological role of this new channel type remains to be elucidated, the combination of  $\text{Na}^+$  permeability, existence of conducting states at negative potentials, and a high conductance, provides an ionic pathway for membrane depolarization in the PC12 cell, even if the density of this channel type in the cellular membrane is low. Preliminary data have been presented in abstract form (Dopico & Treistman, 1997).

## Materials and Methods

### CELL CULTURE

PC12 cells, obtained from Dr. Eric Shooter (Stanford University), were brought up from  $-80^\circ\text{C}$  storage every two months, passaged every week, and their culture medium (*see* composition below) replaced every 2–3 days. Cells were grown on tissue culture dishes (Corning Glass Works, Corning, NY) in Dulbecco's modified Eagle's medium with 3.7 g/l  $\text{NaHCO}_3$ , 25 mM N-2-hydroxyethylpiperazine-N'-2-ethanesulfonate (HEPES)-Na (pH 7.4), 10% heat-inactivated horse serum, 5% fetal bovine serum, 4.5 g/l glucose, 2 mM glutamine, 50 U/ml penicillin G, and 50  $\mu\text{g}/\text{ml}$  streptomycin, in a humidified atmosphere of 10%  $\text{CO}_2$  at  $37^\circ\text{C}$ . Parallel cultures were left untreated or were treated with 50 ng/ml of the 2.5S fraction of NGF (Harlan Bioproducts for Science) for 7–14 days. This procedure induced the growth of neuronal-like processes, with lengths approximately half the diameter of the cell body, evident after 2 days of NGF treatment, as previously described (Mullikin-Kilpatrick & Treistman, 1995). Two days prior to electrophysiological recordings, both undifferentiated and NGF-treated PC12 cells were plated in fresh medium on borosilicate glass coverslips.

### ELECTROPHYSIOLOGICAL RECORDINGS, SOLUTIONS, AND CHEMICALS

Single channel recordings were obtained from excised, inside-out (I/O) and cell-attached (C-A) membrane patches using standard patch-clamp techniques (Hamill et al., 1981). Single channel currents were recorded using a patch-clamp amplifier (EPC7, List Electronics) at a bandwidth of 3 kHz, and low-pass filtered at 1 kHz using an eight-pole Bessel filter (model 902LPF, Frequency Devices, Haverhill, MA). Data were acquired and stored using an A/D converter and an IBM-compatible computer. Electrodes were made as previously described (Dopico, Lemos, & Treistman, 1996). Tip resistances were 6–10 M $\Omega$  when filled with extracellular solution (for composition *see* below). An Ag/AgCl electrode pellet was used as ground electrode. After excision from the cell, the membrane patch was exposed to different bath solutions flowing from a micropipette (1 mm diameter, WPI). All experiments were carried out at room temperature ( $20^\circ\text{C}$ ).

All solutions were made with ultrapure bidistilled water (18 M $\Omega$ ) and with high grade salts. The extracellular (pipette) solution remained constant throughout the experiment, and contained (in mM): 145  $\text{K}^+$  gluconate, 1  $\text{MgCl}_2$ , 5 ethylene glycol-bis-( $\beta$ -aminoethyl ether)-N,N,N',N'-tetraacetic acid (EGTA), 15 HEPES, 10 glucose; pH 7.4. The free  $\text{Ca}^{++}$  concentration ( $[\text{Ca}^{++}]_{free}$ ) was adjusted to 1–10  $\mu\text{M}$  by adding  $\text{CaCl}_2$ . The calculation of the final  $[\text{Ca}^{++}]_{free}$  in all solutions was done according to Fabiato (1988). Gluconate was used to substitute for  $\text{Cl}^-$  due to its extremely low permeability through most anion channels (Shukla & Pockett, 1990; Diaz et al., 1993). In all solutions, the pH was adjusted by addition of the hydroxide of the bulk cation. The intracellular surface of I/O patches was exposed to different (bath) solutions, whose compositions are given in the figure captions. For C-A recordings, the bath solution contained (mM): 145  $\text{K}^+$  gluconate, 1  $\text{MgCl}_2$ , 2.97  $\text{CaCl}_2$ , 5 EGTA, 15 HEPES, 10 glucose; pH 7.4. This high  $\text{K}^+$  solution was used to set the membrane potential close to 0 mV. All tissue culture reagents were obtained from Sigma Chemical, St. Louis, MO. Heat-inactivated horse serum was obtained from J.H.R. Biosciences, Lenexa, KS.

### DATA ANALYSIS

Data acquisition and analysis were performed using pCLAMP software, version 6.0.2 (Axon Instruments). Data were sampled at 3 kHz. The single channel conductance was obtained from the unitary current-voltage relationship ("i/V plot"), which proved to be ohmic in the range of potentials tested ( $-60$  to  $+70$  mV). Unitary current values were obtained from the mean value of the mode in the Gaussian fit of all-points histograms, after leak subtraction. Voltages given correspond to the potential at the intracellular side of the patch (i.e.,  $-V_{pipette}$ ). Potentials have been corrected for offsets due to changes in the  $[\text{Cl}^-]$  of the different bath solutions used.

In ion substitution experiments, the zero-current potential, which was assumed to represent a bionic potential, was used to calculate permeability ratios for monovalent cations ( $P_{A^+}/P_{B^+}$ ) from:  $E_{i=0} = RT/zF \ln (P_A + [A^+]_{oc}/P_B + [B^+]_{ic})$  (Hille, 1992) where subscripts *oc* and *ic* denote external and internal permeant ion species respectively,  $E_{i=0}$  is the zero-current potential, and  $R$ ,  $T$ ,  $z$ , and  $F$  have their usual meaning.

As an index of channel activity we used  $NP_o$ ; i.e., the product of the number of channels present in the patch membrane ( $N$ ) and the probability that a particular channel is open ( $P_o$ ).  $NP_o$  values were calculated from all-points amplitude histograms, assuming a Poisson distribution. In multichannel patches of unknown  $N$ , and in the presence of "overlapping" openings, knowing  $NP_o$ , and the number of openings ( $\#o$ ) during a long period of observation ( $T$ ), allowed calcu-

lation of the mean open time ( $t_o$ ) from the relationship:  $t_o = NP_oT/\#o$  (Fenwick, Marty, & Neher, 1982; Singer & Walsh, 1987); the fact that we obtained only multichannel patches of uncertain  $N$  prevented us from calculating mean closed times. Unless otherwise indicated, data are expressed as mean  $\pm$  SE.

## Results

### CHANNEL IDENTIFICATION; ION CONDUCTION PROPERTIES

In excised, I/O patches from undifferentiated PC12 cells we recorded the activity of ion channels characterized by a large unitary current (Fig. 1). For example, the mean current amplitude of these channel openings using 145 mM  $K^+$  at both sides of the patch was  $13.39 \pm 1.01$  pA (mean  $\pm$  SD of the Gaussian fit) at a holding potential of 40 mV, as assessed from all-points amplitude histograms. Inspection of these traces also shows the presence of at least two functional channels in the patch, and a relatively high channel open probability throughout the range of voltages tested. The channels did not show any noticeable 'run-down' even 20 min after patch excision, in the absence of nucleotides or other 'regenerating' systems in the solutions bathing the patch. The fact that openings were observed in I/O patches several minutes after excision indicates that the continuous presence of freely diffusible extracellular or cytosolic ligands is unnecessary for the channel to dwell in open states. Figure 1 also shows the existence of two subconductance states (*see* arrows), of 90 and 160 pS (calculated from unitary amplitudes obtained from all-points amplitude histograms). The facts that: (i) we never observed these sublevels of current in patches in which we failed to detect the main conductance, (ii) they showed a reversal potential identical to that showed by the main conductance, and (iii) we never observed these sublevels superimposed upon maximal  $NP_o$  of the main conductance, suggest that they represent subconductance levels and are not separate channels coexisting in the same patch. These subconductances were very infrequent (together they typically accounted for less than 5% of the recording), and were not included for analysis.

From data shown in Fig. 1, obtained in symmetric  $K^+$ , it can be seen that current flow through the channels reversed polarity at a membrane potential of about 0 mV. This characteristic would be expected from either large conductance  $Cl^-$ ,  $K^+$ , nonselective cationic, or nonselective anion channels. To minimize the contribution of  $Cl^-$  as carrier of this current, experiments were initially performed (as in the patch depicted in the figure) using both electrode and bath solutions in which gluconate, known to be a very poor permeant of  $Cl^-$  channels (Shukla & Pockett, 1990; Diaz et al., 1993), is substituted for  $Cl^-$  as the main anion. Under these conditions, that is, 145 mM  $K^+$  gluconate (total  $[Cl^-] < 5.7$  mM) at both sides of the

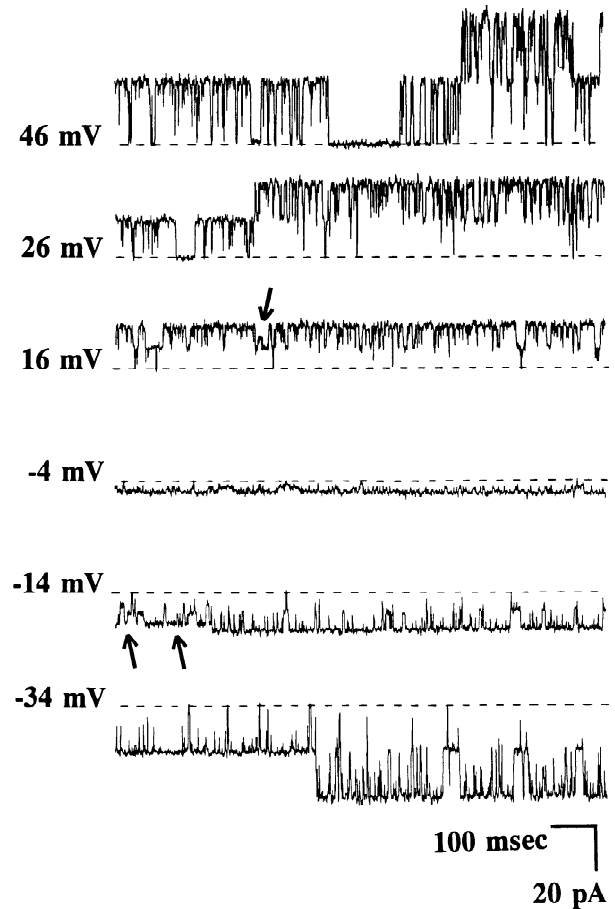


**Fig. 1.** Representative single channel recordings obtained from an excised, inside-out patch of an undifferentiated PC12 cell, in symmetrical  $K^+$  gluconate. The negative of the pipette potential is shown to the left of each trace recorded at a given potential. Outward and inward current through open channels is indicated by upward and downward deflections, respectively. A broken line indicates the baseline (closed channel) level. Arrows indicate infrequent subconductance states (*see* text). The composition of the extracellular (electrode) solution is described in Materials and Methods. The solution facing the intracellular side of the patch (bath solution) contained (mM): 145  $K^+$  gluconate, 1  $MgCl_2$ , 5 EGTA, 15 HEPES, 10 glucose; pH 7.4. The  $[Ca^{++}]_{free}$  was adjusted to  $\approx 1 \mu M$  by adding  $CaCl_2$ . For better quality of display, traces were digitally filtered at 500 Hz.

patch membrane, the single-channel conductance and the reversal potential, obtained from unitary current-voltage relationships (*see* a representative patch in Fig. 2, filled circles-solid line) were  $273.7 \pm 13.56$  pS and  $-0.42 \pm 1.06$  mV ( $n = 6$ ), respectively. When the intracellular side of the patch was exposed to a solution containing 145 mM NaCl, neither the single channel conductance nor the reversal potential were significantly modified:  $270.06 \pm 8.38$  pS and  $-0.8 \pm 0.46$  mV ( $n = 4$ ) (*see* also Fig. 2, hollow circles-dotted line). The facts that: (i) a very large unitary conductance was observed using solutions at both sides of the patch in which almost all the

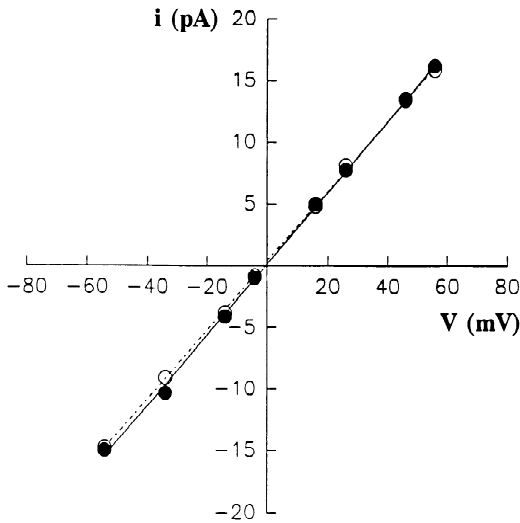


**Fig. 2.** The unitary current-voltage ( $i/V$ ) relationship of the channel under study, measured in the same I/O patch, is unmodified when the bath solution is switched from  $K^+$  gluconate (filled circles, solid line) to NaCl (hollow circles, broken line). Individual points at each potential were determined by computing the mean value of each mode of the all-points amplitude histograms, and plots were fitted using linear regression. The single channel conductance, calculated from slope measurements, and the reversal potential, are 288.8 pS ( $r = 0.998$ ) and  $-0.42$  mV, and 281.5 pS ( $r = 0.996$ ) and  $-1.39$  mV, with  $K^+$  gluconate and NaCl in the bath, respectively. The composition of the electrode solution is described in Materials and Methods. One bath solution contained (mM): 145  $K^+$  gluconate, 1  $MgCl_2$ , 5 EGTA, 15 HEPES, 10 glucose; pH 7.4. The other bath solution contained (mM): 145 NaCl, 1  $MgCl_2$ , 5 EGTA, 15 HEPES, 10 glucose; pH 7.4. In both bath solutions, the  $[Ca^{++}]_{free}$  was adjusted to  $\approx 1 \mu M$  by adding  $CaCl_2$ .

$Cl^-$  was replaced by gluconate and, more important, (ii) there was no shift in the unitary current-voltage relationship toward positive reversal potentials when  $Cl^-$  was substituted for gluconate at the intracellular surface of the patch, indicate that the channels are not noticeably permeable to  $Cl^-$ . In addition, as shown in Fig. 2, the unitary current-voltage relationship for the channel, obtained from I/O patches, remained essentially the same whether  $K^+$  or  $Na^+$  was the sole monovalent cation species in the bath solution, suggesting that the channel shows a similar permeability to  $Na^+$  and  $K^+$ . Indeed, assuming biionic conditions, the permeability ratio  $K^+/Na^+$ , calculated from the zero current potentials was 0.99. On the other hand, when 145 mM LiCl was used in the bath solution, we obtained a permeability ratio  $K^+/Li^+$  of 1.33. In consequence, the current under study can be considered to be underlain by the activity of large conductance, nonselective cation channels that show the following permeability for monovalents:  $K^+ \approx Na^+ > Li^+$ .

#### MODULATION OF CHANNEL ACTIVITY

Large conductance, nonselective cation channels have been described in several preparations. They represent a

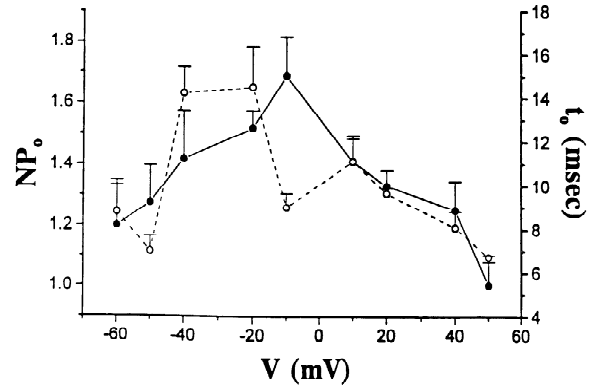


**Fig. 3.** Changes in overall channel activity ( $NP_o$ ) and mean open time as a function of transmembrane voltage.  $NP_o$  values (filled circles) were obtained from all-points amplitude histograms. Mean open time values (hollow circles) from multichannel patches were calculated as described in Materials and Methods. Each point represents the mean  $\pm$  SEM of 4–7 patches. Each patch was obtained from a different cell. All determinations were performed in I/O patches from undifferentiated PC12 cells. The composition of the electrode solution is described in Materials and Methods. The bath solution contained (mM): 145  $K^+$  gluconate, 1  $MgCl_2$ , 5 EGTA, 15 HEPES, 10 glucose; pH 7.4. The  $[Ca^{++}]_{free}$  was adjusted to  $\approx 1 \mu M$  by adding  $CaCl_2$ .

rather heterogenous family whose members can be distinguished based upon the channel response to different modulators, such as transmembrane voltage,  $[Ca^{++}]_{ic}$ , and  $[Na^+]_{ic}$ . For example, large conductance cation channels from peroxisomal membranes (Labarca et al., 1986) or mitochondrial membranes (Thieffry et al., 1988) inserted in lipid bilayers, and a variety of cationic bacterial porins (Benz, 1988), spend most of the time in full-conductance or “open” states at voltages near 0 mV, switching to “closed” states at voltages more negative or more positive than 10–30 mV. In our case, we were able to separately analyze the influence of transmembrane voltage on single channel conductance and channel gating. As we stated above, the two subconductance states that we identified in the present channel were infrequent, accounting together for less than 5% of the area under the curve in the all-points amplitude histograms. This infrequent appearance was similar at all potentials evaluated ( $-60$  to  $50$  mV). On the other hand, the activity ( $NP_o$ ) of the channel under study remained high even at voltages  $> \pm 20$ – $30$  mV (see Fig. 1). However, Fig. 3 (filled circles–solid line) shows that the probability of these channels to be in the open state decreased as a function of voltage symmetrically in both directions, giving a bell-shaped  $NP_o$ –voltage relationship, with maximal activation at about  $-10$  mV.

In all cases, we dealt with multichannel patches in which we could only guess a minimum estimate of  $N$ . Even when the real value of  $N$  is unknown, changes in  $NP_o$  by voltage may be interpreted as changes in  $P_o$ . The possibility that the applied voltage caused a modi-



fication of  $NP_o$  by changing the number of functional channels in the patch is unlikely since we obtained  $NP_o$  values ranging from 1.2 to 1.7 during a long period of time, and across the entire voltage range tested, in which  $NP_o$  was accounted by the overlapping of two opening levels without the appearance of a third level. Thus, changes in channel  $P_o$  by transmembrane voltage account at least in part for voltage-induced changes in channel  $NP_o$ . The increase in channel  $P_o$  at potentials around  $-10$  mV can be explained by an increase in the mean open time ( $t_o$ ), an increase in the frequency of openings (i.e., a decrease in the mean closed time,  $t_c$ ), or both. Even in multichannel patches of unknown  $N$ , and in the presence of "overlapping" openings, knowledge of  $NP_o$ , as well as the number of openings during a long period of observation, allowed us to calculate  $t_o$ , as described in Materials and Methods. The determination of  $t_c$  was not performed, due to the lack of single channel patches. In multichannel patches, the closed intervals that contribute to the mean value may be terminated by the reopening of the channel that closed last or by the opening of another channel, leading to artificially brief  $t_c$  values. Figure 3 (hollow circles-dotted line) illustrates the changes in  $t_o$  as a function of the transmembrane potential. Two areas can be distinguished: at potentials ranging from  $-60$  to  $-10$  mV, changes in  $t_o$  did not parallel, and, therefore, cannot be mainly responsible for, the observed depolarization-induced increase in channel  $NP_o$ . Thus, the ascending limb of the  $NP_o$ -voltage relationship in this negative quadrant mainly results from depolarization-induced decreases in the channel  $t_c$ . On the other hand, at potentials ranging from  $10$  to  $50$  mV,  $t_o$  decreased with membrane depolarization, paralleling the depolarization-induced reduction of  $NP_o$ . Therefore, in the positive quadrant of the  $NP_o$ -voltage relationship, changes in channel  $t_o$  in response to voltage seem to be mainly responsible for voltage-induced changes in channel activity.

A heterogeneous subset of nonselective cation channels is constituted by  $[Ca^{++}]_{ic}$ -activated channels (Siemen, 1993). Among these, a few, like a cationic channel found in peptidergic nerve terminals of the land crab (channel "s"; Lemos et al., 1986), and nonselective cation channels found in vascular smooth muscle cells from different species (Loirand et al., 1991; Mathers & Zhang, 1995), display a unitary conductance similar to that of the channel here reported. We explored the sensitivity of the PC12 nonselective cation channel to  $[Ca^{++}]_{ic}$  by exposing the cytosolic side of I/O patches to different buffered solutions which differed only in the amount of free  $Ca^{++}$ . As shown in Fig. 4A, channel  $NP_o$  was unaffected when the cytosolic side of I/O patches were switched from a  $0$   $Ca^{++}/5$  mM EGTA-containing solution (to chelate trace amount of  $Ca^{++}$ ), to a variety of buffered solutions with increased levels of free  $[Ca^{++}]_{ic}$ , ranging up

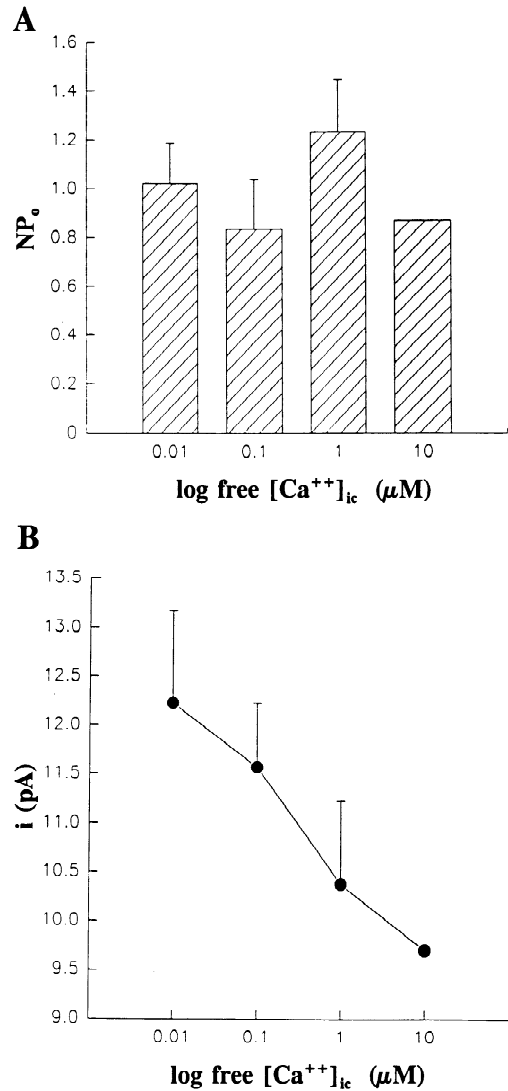


**Fig. 4.** Effect of  $[Ca^{++}]_{ic}$  on channel activity (A) and unitary conductance (B). The intracellular surface of I/O patches was exposed to different bath solutions in which the free  $[Ca^{++}]_{ic}$  was varied. Each point represents the mean  $\pm$  SEM of 3–6 patches. Each patch was obtained from a different cell. All determinations were performed in I/O patches from undifferentiated PC12 cells. The composition of the electrode solution is described in Materials and Methods. The bath solution contained (mM): 145  $K^+$  gluconate, 1  $MgCl_2$ , 5 EGTA, 15 HEPES, 10 glucose; pH 7.4. The  $[Ca^{++}]_{free}$  was adjusted to the values indicated at the bottom of each bar by adding the appropriate amount of  $CaCl_2$ . The membrane potential was set at 40 mV. (A)  $NP_o$  is not affected by changes in the amount of  $[Ca^{++}]_{ic}$ .  $NP_o$  values were obtained from all-points amplitude histograms; (B) The unitary current amplitude of the channel is decreased as the free  $[Ca^{++}]_{ic}$  is increased. Unitary current amplitudes were obtained from all-points amplitude histograms.

to  $\approx 10$   $\mu M$ . Therefore, channel activity was independent of  $[Ca^{++}]_{ic}$  in the range tested, and, by extension, the present channel does not require physiological levels of  $[Ca^{++}]_{ic}$  to dwell in open states. On the other hand, in spite of its lack of effect on channel  $NP_o$ , increasing the

free  $[Ca^{++}]$  at the intracellular side of the patch decreased the unitary current amplitude of the channel, evaluated from all-points amplitude histograms (Fig. 4B). Interestingly, this result is in contrast to results previously reported with  $Ca^{++}$ -activated nonselective cation channels, whether of large (Loirand et al., 1991) or small (Sturgess, Hales, & Ashford, 1987; Gray & Argent, 1990; Thorn & Petersen, 1992) unitary conductance, in which  $[Ca^{++}]_{ic}$  characteristically regulates channel activity without modifying the single channel amplitude. Inspection of our digitally-filtered records (500 Hz; e.g., Fig. 1), as well as those which were not digitally filtered (low-pass filtered at 1 kHz; *data not shown*) indicate that the  $Ca^{++}$ -induced decrease in the apparent unitary amplitude occurred without any noticeable increase in noise at the bandwidth used. Thus, it is not possible to tell from our data whether internal  $Ca^{++}$  inhibits monovalent flux through large conductance, nonselective cation channels in PC12 cells by screening of negative surface charges, rapid open-channel block, or a combination of these possibilities. This result is similar to that reported for the reduction of single channel amplitude of  $Na^+$  channels by divalent cations in rat skeletal muscle (Moczydlowski et al., 1986).

It is widely accepted that nonselective cation channel activity leads to  $Na^+$  entry into the cell. Furthermore, it has been recently demonstrated in PC12 cells that  $Na^+$  entry through nonselective (ATP-activated) cation channels leads to local changes in  $[Na^+]$  that, in turn, inhibit voltage dependent  $K^+$  channels (Strübing & Hescheler, 1996). On the other hand, it has been demonstrated in land crab peptidergic terminals that the activity of a nonselective cation channel is increased by raising the  $[Na^+]_{ic}$  (channel 'f'; Lemos et al., 1986). Therefore, to test a possible modulatory action of  $[Na^+]_{ic}$  on the activity of the channels under study, we evaluated channel  $NP_o$  in the presence of solutions containing either 0, 45, or 145 mM  $Na^+$  at the cytosolic side of I/O patches. This manipulation modified neither the overall channel activity (Fig. 5), nor the channel unitary current (*not shown*). The representative result shown in the figure was replicated in 3 other independent patches.

An important subset of nonselective cation channels are mechano-gated: both stretch-activated (SACs) and stretch-inactivated channels (SICs) that do not markedly discriminate among different monovalent cations have been reported in a wide variety of preparations, with conductances ranging from 7–70 pS (for reviews, *see* Siemen, 1993; Hamill & McBride, 1996). On the other hand, channels of large conductance, such as large conductance,  $Ca^{++}$ -activated  $K^+$  channels has been reported to be activated by suction in excised, I/O patches, under conditions that rule out the mediation of changes in  $[Ca^{++}]_{ic}$  or other freely diffusible second messengers (Kirber et al., 1992; Dopico et al., 1994). The overall

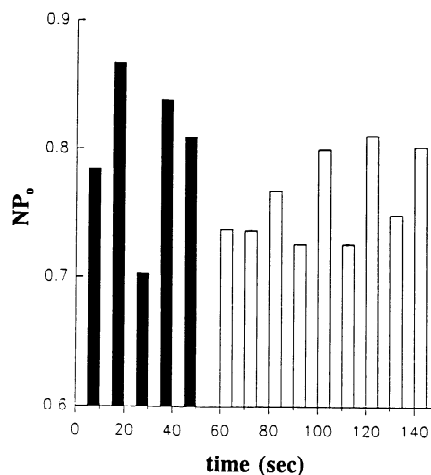


**Fig. 5.** Channel activity ( $NP_o$ ) is not affected by changes in  $[Na^+]_{ic}$ . In a representative experiment, the intracellular surface of an I/O patch was exposed to a bath solution containing 0  $Na^+$  (solid bars), and then switched to a solution containing 145 mM  $Na^+$ .  $NP_o$  values were obtained from all-points amplitude histograms. Each bar corresponds to 10-sec recordings. The composition of the electrode solution is described in Materials and Methods. One bath solution contained (mM): 145  $K^+$  gluconate, 1  $MgCl_2$ , 5 EGTA, 15 HEPES, 10 glucose; pH 7.4. The other bath solution contained (mM): 145  $NaCl$ , 1  $MgCl_2$ , 5 EGTA, 15 HEPES, 10 glucose; pH 7.4. In both bath solutions, the  $[Ca^{++}]_{free}$  was adjusted to  $\approx 1 \mu M$  by adding  $CaCl_2$ . The membrane potential was set at 40 mV. This representative result was confirmed in 3 other patches obtained from different cells.

activity of the channel under study, evaluated in I/O patches exposed to  $Ca^{++}$ -buffered solutions in the absence of nucleotides, increased weakly (20–30%) upon application of suction (50–75 mmHg up to 45 sec) to the back of the patch pipette. In representative traces shown in Fig. 6, average  $NP_o$  increased from 0.92 to 1.19 (+29%) during stretch, and returned to 0.85 upon stopping the suction. This mild increase in channel  $NP_o$  upon application of negative pressure was observed in 4 out of 4 patches. Lower values of suction produced no significant effect on channel  $NP_o$  (*not shown*), whereas higher values routinely resulted in loss of gigaseals. Thus, although some mechanosensitivity may be observed, suction-induced changes in the activity of this channel are much less than those previously reported for SACs, SICs, or large conductance,  $Ca^{++}$ -activated  $K^+$  channels. The application of negative pressure (up to 75 mmHg) to the back of the patch pipette failed to evoke channel openings in previously silent patches ( $n = 7$ ). Whether this failure is due to the fact that the activation of the channel by suction requires some degree of basal (i.e., presuction) channel activity, or simply that these patches lacked the channel protein remains to be established. As previously reported for other mechanogated channels, suction-induced changes in  $NP_o$  occurred without accompanying modifications in unitary conductance. The single channel amplitude of the PC12 cell nonselective

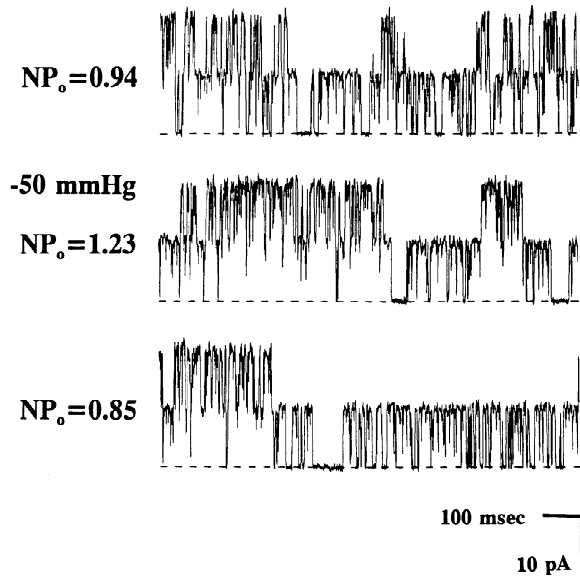


**Fig. 6.** The application of suction to the back of the patch pipette mildly increases channel activity. Representative single channel recordings from an I/O patch before (upper panel), during (middle panel), and after (bottom panel) the application of negative pressure ( $\approx 50$  mmHg) to the back of the patch pipette. Channel openings are shown as upward deflections; a dotted line indicates the baseline.  $NP_o$  values were obtained from all-points amplitude histograms, constructed from 6 sec of recording under each condition. The composition of the electrode solution is described in Materials and Methods. The bath solution contained (mM): 145  $K^+$  gluconate, 1  $MgCl_2$ , 5 EGTA, 15 HEPES, 10 glucose; pH 7.4. The membrane potential was set at 40 mV. This representative result was confirmed in 3 other patches obtained from different cells.

tive cation channel, measured at 40 mV in symmetric 145 mM  $K^+$  was  $13.84 \pm 0.96$ ,  $13.78 \pm 0.93$ , and  $13.46 \pm 1.01$  pA (mean  $\pm$  SD of the Gaussian fit) before, during, and after the application of suction.

#### CHANNEL DENSITY

The number of I/O patches from undifferentiated PC12 cells (each patch was excised from a different cell) in which large conductance, nonselective cation channels were observed, varied among different cell batches: 11 out of 41 patches (26.8%); 1 out of 12 (8.3%), and 4 out of 25 (16%); yielding an overall density of 20.5% (16 out of 78 patches). The reason for this variability is not clear at this time. To determine whether the activity of these channels is evident only in the excised patch situation, we compared channel density in C-A vs. I/O patches, in a single batch of undifferentiated PC12 cells. In the C-A configuration, large conductance, nonselective cation channels were observed in 4 out of 25 patches (16%). After patch excision, the 4 patches with active channels retained channel activity, whereas C-A patches without

functional channels remained silent for the whole period of recording ( $>15$  min). These data indicate that the activity of this channel type is not limited to the artificial situation of the cell-free patch, and suggest that the continued presence of freely diffusible intracellular mediators are not necessary for channel function. Since the common situation was to obtain either patches with no channels at all or multichannel patches with an uncertain  $N$  (therefore, we could only estimate a minimum  $N$ , usually  $N \geq 3$ ), it is reasonable to speculate that this channel type is not evenly distributed, but clustered in the PC12 cell membrane.

As previously, noted, NGF-induced differentiation of PC12 cells has been reported to modify the expression of different types of ion channels. For a particular batch of undifferentiated PC12 cells in which large conductance, nonselective cation channels were found in 11 out of 41 patches (26.8%), channels with identical functional characteristics were found in 6 out of 23 NGF-treated PC12 cells; i.e., 26.1% of patches. These data indicate that NGF-induced differentiation of PC12 cells did not significantly affect the overall density of the channels here described. Since we did not patch the processes in NGF-treated cells, we do not know whether NGF-differentiation affects the distribution of this new channel type in the differentiated cell.

#### Discussion

The results presented in this study demonstrate the presence of a novel, large conductance, nonselective cation channel in PC12 cells. In spite of a unitary conductance similar to that of large conductance,  $Ca^{++}$ -activated  $K^+$  channels, the bell-shaped voltage dependence of channel  $NP_o$  and the lack of activation with increases in  $[Ca^{++}]_{ic}$ , together with the lack of selectivity for  $K^+$  over  $Na^+$ , clearly differentiate the present channel from large conductance,  $Ca^{++}$ -activated  $K^+$  channels, already identified in this clonal cell line (Hoshi & Aldrich, 1988). The fact that we observed a high level of channel activity even 15–20 min after patch excision in the absence of ATP or other nucleotides in the solutions rules out the possibility that the channel characterized here is an ATP-activated, large-conductance nonselective cation channel, known to exist in this and other preparations (Obukhov et al., 1995; Strübing & Hescheler, 1996).

Large conductance, nonselective cation channels constitute a rather heterogenous group of channels, and have been previously reported in a wide variety of systems (for a review, see Siemen, 1993). However, the response of channel activity to different modulators differentiates the present channel type from all other large conductance, nonselective cation channels described, to our knowledge. As shown in Fig. 4A,  $[Ca^{++}]_{ic}$  failed to modulate channel gating. Thus, the present channel is

clearly different from the “s” channel described in crab peptidergic nerve terminals (Lemos et al., 1986), as well as other  $\text{Ca}^{++}$ -activated channels identified in rat portal vein (Loirand et al., 1991), and rat cerebrovascular (Mathers & Zhang, 1995) arteries, which share with the channel characterized here a large unitary conductance and a poor selectivity for  $\text{K}^+$  over  $\text{Na}^+$ . On the other hand, the lack of  $NP_o$  modulation by changes in  $[\text{Na}^+]_i$  (Fig. 5), as well as its higher conductance, differentiates the present channel from the “f” channel described in crab peptidergic nerve terminals (Lemos et al., 1986).

Although the activity of the PC12 channel was reversibly increased by suction without an alteration in its unitary conductance, similar to what is observed with nonselective cation SACs, the present channel differs in major respects from this subset of nonselective cation channels: (i) it displays a high  $P_o$  in the absence of membrane stretch; (ii) it shows a milder increase in activity in response to the applied negative pressure; (iii) it has a much larger unitary conductance.

The bell-shaped  $NP_o$ -voltage relationship displayed by the channel characterized here is similar to the bell-shaped voltage-dependence of gating of a variety of large conductance, nonselective cation channels, such as those from peroxisomal (Labarca et al., 1986) or mitochondrial (Thieffry et al., 1988) membranes inserted in lipid bilayers, and bacterial porins (Benz, 1988). This bell-shaped voltage-dependence of gating is also observed in VDACs and other related anion channels which, due to their capacity to selectively prefer cations over anions under particular conditions (Colombini, 1989; Benz & Brdiczka, 1992), are usually included in the group of large conductance, nonselective cation channels (Siemen, 1993). In all these channels, whether essentially anionic or cationic, the voltage-dependence of gating is underlaid by the fact that the channel (characterized by the existence of multiple conducting states) spends most of the time in full-conductance or “open” states at voltages near 0 mV, and switches to lower conductance or “closed” states at voltages more negative or more positive than 10–30 mV. In the case of VDACs (Marrero et al., 1991; Siemen, 1993), and MIP channels (Modesto et al., 1996), the “switch” to substates is characterized by not only a decrease in conductance from a few nS to hundreds of pS, but also a change from anion to cation selectivity (Colombini, 1989; Benz & Brdiczka, 1992). In contrast, the channel described in this study did not show any noticeable permeability for  $\text{Cl}^-$ . In addition, its voltage-dependence of gating is not explained by a “switch” to substates, but essentially by the voltage-dependence of the open probability of the main conductance state. This voltage dependence of channel  $NP_o$  seems to be accounted for by the voltage-dependence of channel  $t_o$  only in the positive quadrant of the  $NP_o$ -voltage relationship. Since we did not evaluate the dis-

tribution of open or closed times due to the lack of single channel patches, gating schemes that may provide some insight into this asymmetry in the voltage dependence of  $t_o$  have yet to be established. Finally, the combination of impermeability to  $\text{Cl}^-$  and the bell-shaped  $NP_o$ -voltage relationship differentiates the channel characterized here from hyperpolarization-activated, large conductance nonselective channels, such as those described in bovine pigmented ciliary epithelial cells (Mitchell & Jacob, 1996).

As with many other members of the heterogenous family of nonselective cation channels, the function of the new channel type found in PC12 cells remains speculation. It is interesting to note that channel activity was still observed several minutes after patch excision, which indicates that the channel does not require the presence of any freely diffusible extracellular or cytosolic messenger to be open. Nevertheless, it is possible that one or more freely diffusible ligands (either extracellular or cytosolic) are needed to gate the channel into nonconducting states. For example, nonselective cation channels inhibited by intracellular ATP or ADP have been described in pancreatic duct (Gray & Argent, 1990) and acinar cells (Thorn & Petersen, 1992). Similarly, AMP, ADP, ATP, and cAMP, as well as other nucleotides, applied to the intracellular surface of I/O patches reduced the activity of nonselective cation channels in CRI-G1 cells (Sturgess, Hales, & Ashford, 1987; Reale, Hales, & Ashford, 1994, 1995). All these nonselective cation channels are characterized by a similar unitary conductance (25 pS), more than 10 times smaller than that of the channel reported here. The PC12 channel passes  $\text{Na}^+$  and  $\text{K}^+$ , but not  $\text{Cl}^-$ , and under physiological conditions would be expected to conduct mainly  $\text{Na}^+$  into the cell, resulting in depolarization. The total current ( $I$ ) flowing through a patch is a function of different factors:

$$I = f(NP_o)i$$

where  $N$ : number of functional channels present in the patch;  $P_o$ : the probability of a channel being open;  $i$ : unitary current amplitude. The unitary current amplitude of this channel at the normal resting potential in PC12 cells ( $\approx -50$  mV; O’Lague & Huttner, 1980) would be on the order of 13.5 pA. Considering an average  $NP_o$  of 1.2 at that potential (*see* Fig. 3), the mean percentage of active patches observed ( $\approx 20.5\%$ ) and an average patch area of  $\approx 6 \mu\text{m}^2$ , we can estimate 3.3 pA of inward current per  $6 \mu\text{m}^2$  of cell surface area. The diameter of undifferentiated PC12 cells varies from 8–12  $\mu\text{m}$  (Greene & Tischler, 1976). Therefore, assuming spherical geometry, the surface area of undifferentiated PC12 cells can be estimated at a minimum value (i.e., without considering possible surface folding) of  $314.2 \mu\text{m}^2$ . Then, considering a resting membrane resistance of 0.1  $\text{G}\Omega$ , the simultaneous activation of only a fraction of the



total channel population would result in  $\text{Na}^+$  currents of a magnitude sufficient to drive the membrane potential  $\approx 17$  mV in a depolarizing direction away from rest. This depolarization would eventually contribute to triggering action potentials, and activation of voltage-dependent  $\text{Ca}^{++}$  channels, resulting in an increase in cytosolic  $[\text{Ca}^{++}]$ . In turn, depolarization and increases in cytosolic  $[\text{Ca}^{++}]$  have been reported to be critical in a variety of physiological processes in PC12 cells, such as differentiation (Saffell, Walsh, & Doherty, 1992; Solem, McMahon, & Messing, 1995), and release of catecholamines (Shafer & Atchison, 1991). In addition, local changes in  $[\text{Na}^+]_{ic}$  due to  $\text{Na}^+$  influx through large conductance, ATP-dependent nonselective cation channels have been recently demonstrated to regulate the activity of voltage-dependent  $\text{K}^+$  channels in PC12 cells (Strübing & Hescheler, 1996). Interestingly, given the wide-ranging consequences that might result from activation of the large conductance channel described here, the unitary current amplitude of the present channel decreases as  $[\text{Ca}^{++}]$  at the cytosolic side of the patch increases, and channel  $NP_o$  decreases as the voltage moves away from  $-10$  mV towards more positive values, possibly representing negative feed-back mechanisms to limit depolarization and increases in  $[\text{Ca}^{++}]_{ic}$ .

In conclusion, we have identified, in both undifferentiated and NGF-treated PC12 cells, a novel large conductance, nonselective cation channel. Its existence must be considered when patch-clamp studies on other large conductance channels, such as large conductance,  $\text{Ca}^{++}$ -activated  $\text{K}^+$  channels, are performed in this cell line using symmetric  $[\text{K}^+]$  solutions. The combination of large unitary conductance and  $\text{Na}^+$  permeability, coupled with the voltage and  $[\text{Ca}^{++}]_{ic}$  modulation of the current that passes through this channel, suggest that this new type of channel may play a significant physiological role in cells in which it is expressed.

We wish to thank Dr. Debra Mullikin-Kilpatrick for cell cultures, and Andy Wilson for excellent technical assistance. This work was supported by grants from the Alcoholic Beverage Medical Research Foundation (AMD) and National Institutes of Health AA05512 (SNT).

## References

- Benz, R. 1988. Structure and function of porins from gram-negative bacteria. *Ann. Rev. Microbiol.* **42**:359–393
- Benz, R., Brdiczka, D. 1992. The cation-selective substate of the mitochondrial outer membrane pore: single channel conductance and influence on intermembrane and peripheral kinases. *J. Bioenerg. Biomembr.* **24**:33–39
- Colombini, M. 1989. Voltage gating in the mitochondrial channel, VDAC. *J. Membrane Biol.* **111**:103–111
- Diaz, M., Valverde, M.A., Higgins, C.F., Rucăreanu, C., Sepúlveda, F.V. 1993. Volume-activated chloride channels in HeLa cells are blocked by verapamil and dideoxyforskolin. *Pfluegers Arch.* **422**:347–353
- Dopico, A.M., Kirber, M.T., Singer, J.J., Walsh, J.V., Jr. 1994. Membrane stretch directly activates large conductance  $\text{Ca}^{++}$ -activated  $\text{K}^+$  channels in smooth muscle cells freshly dissociated from rabbit mesenteric artery. *Am. J. Hypertension* **7**:82–89
- Dopico, A.M., Lemos, J.R., Treistman, S.N. 1996. Ethanol activates large-conductance,  $\text{Ca}^{++}$ -activated  $\text{K}^+$  channels in neurohypophysial terminals. *Mol. Pharmacol.* **49**:40–48
- Dopico, A.M., Treistman, S.N. 1997. A novel large conductance, non-selective cation channel in undifferentiated PC12 cells. *Biophys. J.* **72**:A271
- Evans, R.J., Lewis, C., Buell, G., Valera, S., North, R.A., Surprenant, A. 1995. Pharmacological characterization of heterologously expressed ATP-gated cation channels (P2x purinoceptors). *Mol. Pharmacol.* **48**:178–183
- Fabiato, A. 1988. Computer programs for calculating total from specified free or free from specified total ionic concentrations in aqueous solutions containing multiple metals and ligands. In: *Methods in Enzymology, Biomembranes*, vol. 157: ATP-driven pumps and related transport. F. Fleischer and B. Fleischer, editors. pp. 378–417, Academic Press, San Diego
- Fanger, G.R., Brennan, C., Henderson, L.P., Gardner, P.D., Maue, R.A. 1995. Differential expression of sodium channels and nicotinic acetylcholine receptor channels in nnr variants of the PC12 pheochromocytoma cell line. *J. Membrane Biol.* **144**:71–80
- Fenwick, E.M., Marty, A., Neher, E. 1982. Sodium and calcium channels in bovine chromaffin cells. *J. Physiol.* **331**:599–635
- Garber, S.S., Hoshi, T., Aldrich, R.W. 1989. Regulation of ionic currents in pheochromocytoma cells by nerve growth factor and dexamethasone. *J. Neurosci.* **9**:3976–3987
- Gray, M.A., Argent, B.E. 1990. Nonselective cation channel on pancreatic duct cells. *Biochim. Biophys. Acta* **1029**:33–42
- Greene, L.A., Tishler, A.S. 1976. Establishment of a noradrenergic clonal line of rat adrenal pheochromocytoma cells which respond to nerve growth factor. *Proc. Natl. Acad. Sci. USA* **73**:2424–2428
- Hamill, O.P., Marty, A., Neher, E., Sackmann, B., Sigworth, F.J. 1986. Improved patch-clamp techniques for high-resolution current recording from cells and cell-free membrane patches. *Pfluegers Arch.* **391**:85–100
- Hamill, O.P., McBride, D.W. 1996. The pharmacology of mechanogated membrane ion channels. *Pharmacol. Reviews* **48**:231–252
- Hille, B. 1992. *Ionic channels of excitable membranes*. Sinauer, Sunderland, MA
- Hoshi, T., Aldrich, R.W. 1988. Voltage-dependent  $\text{K}^+$  currents and underlying single  $\text{K}^+$  channels in pheochromocytoma cells. *J. Gen. Physiol.* **91**:73–106
- Kirber, M.T., Ordway, R.W., Clapp, L.H., Walsh, J.V., Jr., Singer, J.J. 1992. Both membrane stretch and fatty acids directly activate large conductance  $\text{Ca}^{++}$ -activated  $\text{K}^+$  channels in vascular smooth muscle cells. *FEBS Lett.* **297**:24–28
- Labarca, P., Wolff, D., Soto, U., Necochea, C., Leighton, F. 1986. Large cation-selective pores from rat liver peroxisomal membranes incorporated to planar lipid bilayers. *J. Membrane Biol.* **94**:285–291
- Lemos, J.R., Nordmann, J.J., Cooke, I.M., Stuenkel, E.L. 1986. Single channels and ionic currents in peptidergic nerve terminals. *Nature* **319**:410–412
- Lewis, D.L., De Aizpurua, H.J., Rausch, D.M. 1993. Enhanced expression of  $\text{Ca}^{2+}$  channels by nerve growth factor and the v-src oncogene in rat pheochromocytoma cells. *J. Physiol.* **465**:325–342
- Loirand, G., Pacaud, P., Baron, A., Mironneau, C., Mironneau, J. 1991. Large conductance calcium-activated non-selective cation channel in smooth muscle cells isolated from rat portal vein. *J. Physiol.* **437**:461–475
- Marrero, H., Orkand, P.M., Kettenmann, H., Orkand, R.K. 1991.

- Single-channel recording from glial cells on the untreated surface of the frog optic nerve. *Eur. J. Neurosci.* **3**:813–819
- Mathers, D.A., Zhang, X. 1995. Nonselective cation channels in cerebrovascular smooth muscle cells of adult rats. *Biochim. Biophys. Acta* **1236**:89–94
- Mitchell, C.H., Jacob, T.J.C. 1996. A nonselective high conductance channel in bovine pigmented ciliary epithelial cells. *J. Membrane Biol.* **150**:105–111
- Moczydlowski, E., Uehara, A.S., Guo, X., Heiny, J. 1986. Isochannels and blocking modes of voltage-dependent sodium channels. *Ann. N.Y. Acad. Sci.* **479**:269–292
- Modesto, E., Lampe, P.D., Ribeiro, M.C., Spray, D.C., Campos de Carvalho, A.C. 1996. Properties of chicken lens MIP channels reconstituted into planar lipid bilayers. *J. Membrane Biol.* **154**:239–249
- Mullikin-Kilpatrick, D., Treistman, S.N. 1995. Inhibition of dihydropyridine-sensitive  $Ca^{++}$  channels by ethanol in undifferentiated and nerve growth factor-treated PC12 cells: Interaction with the inactivated state. *J. Pharmacol. Exp. Ther.* **272**:489–497
- Obukhov, A.G., Jones, S.V.P., Degtiar, V.E., Lückhoff, A., Schultz, G., Hescheler, J. 1995.  $Ca^{2+}$ -permeable large-conductance nonselective cation channels in rat basophilic leukemia cells. *Am. J. Physiol.* **269**:C1119–C1125
- O'Lague, P.H., Huttner, S.L. 1980. Physiological and morphological studies of rat pheochromocytoma cells (PC12) chemically fused and grown in culture. *Proc. Natl. Acad. Sci. USA* **77**:1701–1705
- Pollock, J.D., Krempin, M., Rudy, B. 1990. Differential effects of NGF, FGF, ECF, cAMP, and dexamethasone on neurite outgrowth and sodium channel expression in PC12 cells. *J. Neurosci.* **8**:2626–2637
- Reale, V., Hales, C.N., Ashford, M.L.J. 1994. Nucleotide regulation of a calcium-activated cation channel in the rat insulinoma cell line, CRI-G1. *J. Membrane Biol.* **141**:101–112
- Reale, V., Hales, C.N., Ashford, M.L.J. 1995. Regulation of calcium-activated nonselective cation channel activity by cyclic nucleotides in the rat insulinoma cell line, CRI-G1. *J. Membrane Biol.* **145**:267–278
- Saffell, J.L., Walsh, F.S., Doherty, P. 1992. Direct activation of second messenger pathways mimics cell adhesion molecule-dependent neurite outgrowth. *J. Cell. Biol.* **118**:663–670
- Sands, S.B., Barish, M.E. 1992. Neuronal nicotinic acetylcholine receptor currents in pheochromocytoma (PC12) cells: dual mechanisms of rectification. *J. Physiol.* **447**:467–487
- Schmid-Antomarchi, H., Hugues, M., Lazdunski, M. 1986. Properties of the apamin-sensitive  $Ca^{2+}$ -activated  $K^{+}$  channel in PC12 pheochromocytoma cells which hyperproduce the apamin receptor. *J. Biol. Chem.* **261**:8633–8637
- Shafer, T.J., Atchison, W.D. 1991. Transmitter, ion channel and receptor properties of pheochromocytoma (PC12) cells: A model for neurotoxicological studies. *Neurotoxicol.* **12**:473–492
- Shukla, H., Pockett, S. 1990. A chloride channel in excised patches from cultured rat hippocampal neurons. *Neurosci. Lett.* **112**:229–233
- Siemen, D. 1993. Nonselective cation channels. In: Nonselective Cation Channels: Pharmacology, Physiology and Biophysics. D. Siemen and J. Hescheler, editors. pp. 3–25. Birkhauser Verlag, Switzerland
- Singer, J.J., Walsh, Jr., J.V. 1987. Characterization of calcium-activated potassium channels in single smooth muscle cells using the patch-clamp technique. *Pfluegers Arch.* **408**:98–111
- Solem, M., McMahon, T., Messing, R.O. 1995. Depolarization-induced neurite outgrowth in PC12 cells requires permissive, low level NGF receptor stimulation and activation of calcium/calmodulin-dependent protein kinase. *J. Neurosci.* **15**:5966–5975
- Streit, J., Lux, H.D. 1987. Voltage dependent calcium currents in PC12 growth cones and cells during NGF-induced cell growth. *Pfluegers Arch.* **408**:634–641
- Strübing, C., Hescheler, J. 1996. Potassium current inhibition by nonselective cation channel-mediated sodium entry in rat pheochromocytoma (PC-12) cells. *Biophys. J.* **70**:1662–1668
- Sturgess, N.C., Hales, C.N., Ashford, M.L.J. 1987. Calcium and ATP regulate the activity of a non-selective cation channel in a rat insulinoma cell line. *Pfluegers Arch.* **409**:607–615
- Tewari, K., Simard, J.M., Peng, Y.B., Werrbach-Perez, K., Perez-Polo, J.R. 1995. Acetyl-L-carnitine arginyl amide (ST857) increases calcium channel density in rat pheochromocytoma (PC12) cells. *J. Neurosci. Res.* **40**:371–378
- Thieffry, M., Chich, J-F., Goldschmidt, D., Henry, J-P. 1988. Incorporation in lipid bilayers of a large conductance cationic channel from mitochondrial membranes. *EMBO J.* **7**:1449–1454
- Thorn, P., Petersen, O.H. 1992. Activation of nonselective cation channels by physiological cholecystokinin concentrations in mouse pancreatic acinar cells. *J. Gen. Physiol.* **100**:11–25